

solid-state language). That fact that the coupling is smaller *but not 0* appears to imply that the hole is not in a pure 1S state.

The hole-burning technique is necessary because the sample is a mixture of different crystallites. Advances in synthesis that narrow the distribution of sizes and isomers and eliminate electron-hole recombination sites (by eliminating random defects in the structure) directly reflect themselves in an improvement in spectra and photophysics. The upper panel of Figure 8 shows the spectrum³⁴ of the wurtzite CdSe particles whose X-ray powder pattern appears in Figure 5. The HOMO-LUMO transition is sharper than that in Figure 7. In the hole-burning spectrum, the second lowest 1S-1S type transition and a new small peak, C, are also resolved. The HOMO-LUMO transition can be $\approx 90\%$ bleached in Figure 8, while only $\approx 10\%$ bleached in Figure 7. Thus the wurtzite particles *all* have nanosecond or longer excited-state lifetimes, while most of the Figure 7 particles have much shorter lifetimes, presumably due to the presence of structural defects.

In the excited state, the 1S-type (i.e., HOMO-LUMO) absorptions bleach, and there is broad transient optical absorption shifted to higher energy. The bleaching of the 1S transitions is expected for an excited state having both the electron and the hole delocalized

(34) Bawendi, M. G.; Rothberg, L.; Wilson, W.; Carroll, P.; Djeu, N.; Brus, L., to be published.

inside the crystallite and also should occur for surface-trapped carriers.³⁵ The dynamics of these spectroscopic changes, together with the accompanying luminescence, reflect in some way the localization and reorganization of the wave function after optical excitation. This area of research is under active current investigation.

Conclusion and Outlook

Synthesis, characterization, and theory are now approaching the point where study of large semiconductor clusters is a quantitative branch of chemistry. The fundamental ideas involved are the same as those that underlie all of chemistry. This Account discusses recent progress, as well as present needs, either for further synthetic invention or for further physical understanding. It is especially intriguing that these large molecules combine phenomena that normally are associated with separate disciplines: surface science, solid-state physics, molecular electronic spectroscopy, and molecular synthesis.

We deeply appreciate collaboration with many colleagues whose names appear in the references. The supportive and stimulating environment within AT&T Bell Laboratories made this research possible. We are thankful to A. Lovinger and F. Padden for graciously allowing the use of electron microscope facilities.

(35) Hilinski, E.; Lucas, P.; Wang, Y. *J. Chem. Phys.* 1988, 89, 3435.

Role of Mass Transport in Laser-Induced Chemistry

TOIVO T. KODAS

Department of Chemical and Nuclear Engineering, The University of New Mexico, Albuquerque, New Mexico 87131

PAUL B. COMITA*

IBM Almaden Research Center, 650 Harry Road, San Jose, California 95120

Received August 4, 1989 (Revised Manuscript Received March 23, 1990)

The use of laser light to selectively drive chemical reactions on a micron scale is an extremely rapidly evolving technology. Laser light can be used as a source of local heating on a solid surface in order to accelerate surface reactions, or alternatively it can provide radiation of an appropriate wavelength to drive a photochemical reaction in a localized region, either above or

Toivo Kodas received his Ph.D. with Sheldon Friedlander from the University of California, Los Angeles in 1986. He was a Visiting Scientist at IBM Research Division, Almaden Research Center in San Jose until 1988, when he joined the University of New Mexico as an assistant professor of chemical engineering. His research interests include photon-assisted processing of materials, chemical vapor deposition, processing of superconducting ceramics, and aerosol physics and chemistry.

Paul B. Comita is presently a research staff member at IBM Almaden Research Center. He received his undergraduate degree in chemistry from Lawrence University in Appleton, WI, and he received his Ph.D. in chemistry from the University of California, Berkeley in 1981, for his work in the area of vibrationally excited states and infrared laser multiphoton dissociation with Professor R. G. Bergman. After postdoctoral work at Stanford University with Professor John I. Brauman, he joined the IBM Research Division. His primary research interests are in the areas of laser-induced surface phenomena and laser diagnostic techniques.

at the gas-solid interface. The ability to focus light beams to diameters on the order of microns allows the high-resolution patterning of materials, which can be useful in the fabrication of high-density microelectronic circuitry. In addition, laser technology has made an impact on many new processes because materials can be deposited or removed at lower temperatures and with higher rates than can be obtained with conventional processes.¹

A unique aspect of driving chemical reactions in a localized region is size effects that can influence the kinetics of reaction phenomena by influencing gas-phase transport of atomic and molecular species. Mass-transport kinetics are important in photochemical and thermal deposition, etching, and cluster- or particle-formation processes. In conventional chemical vapor deposition (CVD), the overall rate of the deposition

(1) See for example: *Laser Microfabrication: Thin Film Processes and Lithography*; Ehrlich, D. J., Tsao, J. Y., Academic Press: San Diego, CA, 1989.

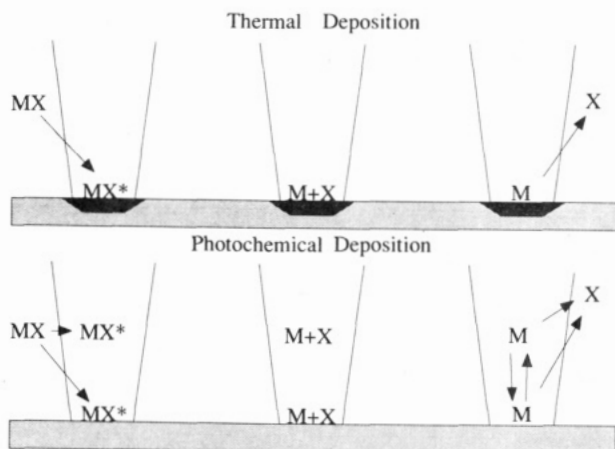


Figure 1. Reaction and transport phenomena taking place during thermal and photochemical deposition. In thermal deposition, the reactant migrates to the zone on the surface heated by the laser beam, reaction takes place, and byproducts migrate away. In photochemical deposition, reaction can take place either on the surface or in the gas. The product can migrate to the surface, leading to film formation, or cluster in the gas phase, leading to particle formation.

reaction can be controlled by the rate of gas-phase or surface reactions, or by the rates of reactant and product transport in the gas phase. For laser-driven reactions, such as laser-induced chemical vapor deposition (LCVD), the relative importance of reaction and transport in determining the overall rate is influenced by the geometry of the deposition apparatus, the laser beam focal spot diameter, and the mean free path of the gas that surrounds the reaction zone. The large difference in the characteristic dimensions of laser-driven and conventional large-area CVD processes leads to the wide differences in deposition rates. Maximum rates on the order of $1000 \mu\text{m/s}$ are possible with LCVD; in comparison, rates are many orders of magnitude lower for large-area processes. High rates are critical in one of the primary uses of LCVD, the direct writing of micron-sized spots and lines onto surfaces, for applications such as mask and circuit repair and the generation of custom gate arrays. In these applications, maximizing the deposition rate is one of the primary goals, because the direct-write process involves serial deposition of lines rather than parallel deposition as in lithographic processes.

Laser-induced surface reactions, such as LCVD, proceed via a sequence of physical and chemical reaction steps beginning with the transport of reactant to the surface of the reaction zone (see Figure 1). The reactant adsorbs and either reacts, producing an atom of the depositing material and other products, or desorbs. The reaction product desorbs if the energy of desorption is sufficiently low, and subsequently migrates away from the surface. Atoms formed on the surface can nucleate to form clusters. The growth kinetics during the nucleation regime is highly nonlinear because the adsorption and activation energies for the surface reactions enter as exponential terms in the rate expressions. The importance of the nucleation step in influencing the overall rate of film growth depends on whether spots or lines are being formed. The deposition of a spot involves the formation of nuclei on the surface of the substrate, growth and coalescence of the nuclei to form a continuous deposit, and further growth of the

continuous deposit to its final size. In contrast, during deposition of lines, the nucleation process either is eliminated or takes place simultaneously with the growth stage, and a kinetic description of this process is much more complicated. The results in this paper will therefore be restricted to the situation wherein a continuous deposit has been formed, and the kinetics of heterogeneous nucleation does not influence the overall growth kinetics. The results also do not take into account explicitly a time-dependent surface-temperature profile, which must be accounted for in many physically realistic situations, such as systems wherein the optical and thermal properties of the substrate are being modified by the deposit.² Heterogeneous transport phenomena in which mass transport occurs between a pair of solid surfaces, as is the case in some plasma-assisted etching and deposition processes,³ is beyond the scope of this Account.

Transport Phenomena

Many of the fundamental issues that are key to our understanding of rate phenomena involved in reactions driven by focused lasers have analogies in the field of aerosol particle growth,⁴ where transport on submicron and micron scales often determines rates of particle growth. Transport processes can in general occur by a molecular-bombardment (ballistic) mechanism in the free-molecular-flow regime, or a diffusive mechanism in the viscous-flow regime. The relative importance of ballistic and diffusive transport depends on the Knudsen number, Kn , the ratio of the gas mean free path to the characteristic dimension of the system.⁴⁻⁶

Many laser-induced deposition processes are operated with sufficiently low pressures (1 Torr or less) and sufficiently small laser focal spot diameters ($1-10 \mu\text{m}$) that $Kn \gg 1$. In this case, no concentration gradients occur in the gas phase, and the reactants and products are transported to and from the surface by a ballistic mechanism. The departure of product molecules from the surface does not influence the arrival of the reactant species at the surface. This situation corresponds to surface-reaction-controlled operation. If, however, the surface reaction is very efficient, the reaction rate is limited by the rate of reactant transport to the deposit surface by molecular bombardment. Ballistic transport theory then provides an estimate of the maximum deposition rate.⁴⁻⁶

Another mode of operation for laser-driven reactions is the situation where $Kn \ll 1$ and transport occurs by a diffusive mechanism. This type of operation occurs for systems wherein high pressures and a large reaction zone are employed. In the general case, thermal and photochemical reactions occur both on the surface and in the gas phase. Products formed in the gas phase leave the reaction zone or may collide to form clusters. Thus, many physical processes can influence the reaction rate, including diffusion of reactants and products, gas-phase reactions, surface reactions, and gas-phase

(2) Kodas, T. T.; Baum, T. H.; Comita, P. B. *J. Appl. Phys.* **1987**, *61*, 2749.

(3) Zarowin, C. B. *J. Appl. Phys.* **1985**, *57*, 929.

(4) Friedlander, S. K. *Smoke, Dust and Haze*; Wiley Interscience: New York, 1977; p 252.

(5) Hidy, G. M.; Brock, J. R. *The Dynamics of Aerocolloidal Systems*; Pergamon: New York, 1970.

(6) Seinfeld, J. H. *Atmospheric Chemistry and Physics of Air Pollution*; Wiley: New York, 1986.

Table I
Summary of Deposition Rate Expressions

mechanism	transport regime	deposition rate (da/dt) ^a	eq no.
thermal	molecular bombardment ($a \ll l$) or surface reaction ^b ($\alpha \ll 1$)	$\frac{\alpha v_1 p_1}{(2\pi mkT)^{1/2}}$	2
	diffusion ($a \gg l$)	$\frac{D_{AB} v_1 p_1}{akT}$	4
	molecular bombardment, transition ($a \sim l$), and diffusion	$\frac{\alpha v_1 p_1}{(2\pi mkT)^{1/2}} \left(\frac{4(Kn)/3\alpha}{1 + 4(Kn)/3\alpha} \right)$	6
photochemical	molecular bombardment ($a \ll l$)	$\frac{\alpha_s \sigma P v_1 p_1}{2(2\pi)^{1/2} h \nu a k T}$	8
	diffusion ($a \gg l$)	$\frac{\alpha_s \sigma P v_1 p_1}{(2\pi)^{1/2} h \nu a k T}$	9

^a In these equations, a is the radius of the deposit, l is the gas mean free path, v_1 is the volume of an atom in the deposit, p_1 is the partial pressure of the deposit precursor, m is the molecular mass of the precursor, α is the fraction of collisions resulting in reaction, P is the laser power, σ is the photodecomposition cross section, and α_s is the sticking probability of the atom produced by reaction. ^b This expression is valid for all deposit sizes.

cluster formation. Using Fick's second law, the governing equation for the concentration of a species that is formed by chemical reaction can be written in cylindrical coordinates, r and z , as

$$\frac{\partial c}{\partial t} + v_r \frac{\partial c}{\partial r} + v_z \frac{\partial c}{\partial z} = D_{AB} \left(\frac{1}{r} \frac{\partial}{\partial r} \left(r \frac{\partial c}{\partial r} \right) + \frac{\partial^2 c}{\partial z^2} \right) + R_+ - R_- \quad (1)$$

where c is the concentration of product, D_{AB} is the effective binary diffusion coefficient, R_+ is the net rate of formation of product by chemical reaction, R_- is the net loss of product to cluster formation, and v_r and v_z are velocities in radial and axial directions, respectively. This equation applies to both thermally and photochemically driven reactions and can be coupled to equations describing the temperature profiles in the substrate and the gas. Depending on the length scales of the system, free and forced convection (gas flow) may also be important and can be described by a momentum transport equation. An equation similar to the one above for a reaction product can be written for other products and for the reactants. Surface reactions of adsorbed species enter the problem through the boundary conditions.

Free-Molecular-Flow Regime

The transport-limited deposition rate for the case wherein the reaction probability α is sufficiently large and $Kn \gg 1$ can be calculated by using kinetic theory.⁷ This expression (eq 2 in Table I) is somewhat different from the expression used by Ehrlich and Tsao⁸ to describe deposition for $Kn \gg 1$. The deposition rate is the same in the absence or presence of buffer gas provided that there is no change in the surface-reaction rate as buffer gas is added. Equation 2 in Table I shows that the deposition rate is linearly dependent on the partial pressure of the deposit precursor (p_1), but is independent of the partial pressure of the buffer gas. The rate cannot be increased by raising the temperature at

the surface, but it can be increased by raising the rate of reactant transport to the surface by increasing the reactant partial pressure.

The reaction probability, α , is a parameter that embodies the influence of many sequential surface processes. A reactant molecule must first impinge on the deposit surface and then stick. The fraction of molecules that stick has been called the trapping coefficient.⁹ The reactant molecule may then diffuse to a site where it is chemically or physically adsorbed. The adsorbed reactant may then desorb, or it may react, followed by desorption of the products. If the rates of the surface processes are fast relative to the rate at which molecules arrive on the surface and desorption of reactant is negligible, the reaction probability becomes equal to the trapping probability. The trapping probability is a weak function of the surface temperature for many species and is often of order 1.¹⁰ Therefore, the deposition rate and the value of α for reactant-transport-controlled deposition of a spot depend only weakly on the surface temperature. In contrast, deposition rates and values of α for surface-reaction-controlled processes depend strongly on temperature, and values of α are usually much less than 1. Hence, the value of α is indicative of the rate-determining step for deposition.

Continuum Regime

For a sufficiently high pressure of the reactant or with a high buffer-gas pressure, as discussed above, $Kn \ll 1$ and mass transport takes place by a diffusive mechanism. If the surface reaction is sufficiently rapid, concentration gradients will exist in the gas phase, and the deposition rate will be limited by the rate of mass transport in the gas phase. In this case, eq 1 or the corresponding equation in spherical coordinates can be used to describe the deposition process. Solutions to eq 1 have been obtained for various limiting cases. A number of analytical solutions have been published for the spherically symmetric problem assuming no convection and no gas-phase reactions.^{7,8,11,12} However, few

(7) Kodas, T. T.; Baum, T. H.; Comita, P. B. *J. Appl. Phys.* 1987, 62, 281.

(8) Ehrlich, D. J.; Tsao, J. Y. *J. Vac. Sci. Technol.*, B 1983, 1, 969.

(9) Boudart, M.; Djega-Mariadassou, G. *Kinetics of Heterogeneous Catalytic Reactions*; Princeton University Press: Princeton, NJ, 1984; p 44.

(10) Weinberg, W. H.; Merrill, R. P. *J. Vac. Sci. Technol.* 1971, 8, 718.

of these theoretical studies have attempted to provide a general theoretical framework for the process.⁷ It is instructive to consider three cases for mass-transport-limited deposition. In the first case, a single reactant is transported to a surface where it reacts, but forms no volatile products. In the second case, one or more gaseous products are formed as the result of chemical reaction. In the third case, buffer gas is present in excess over the reactant and products.

In the first case, with the absence of buffer gas, no species desorb and the surface is a perfect sink for the reactant molecule. This single-component system is equivalent to condensation, where $A(g) \rightarrow A(s)$. Examples of chemically reactive systems such as this include polymerization reactions. For these cases, mass transport to the surface for the undiluted reacting molecule $A(g)$ is described by eq 2 (Table I). Transport takes place by free molecular flow and not diffusion. The validity of eq 2 for this case has been experimentally demonstrated.¹³

In the second case for undiluted reactant gas, reaction products are formed and desorb. This case is the most common situation for LCVD. For the deposition of metals and semiconductors, the reactant normally contains a metal or semiconductor atom plus ligands. The products formed from the ligands and any co-reactant gases must desorb after reaction, in order to form a pure deposit. Similarly, in a laser-induced etching reaction, the reactants must form products that are easily desorbed, in order to remove material rapidly.

The simplest case of undiluted reactant gas is the surface reaction to form a solid species and one gaseous product, i.e., $A(g) \rightarrow B(s) + C(g)$. For this case, the solution to the mass-transport equation (eq 1) is identical with the case with diffusion through an inert buffer gas with any number of gaseous products so long as the concentration of the products is much less than that of the buffer gas. This is because, for both cases, there is effectively no transport occurring due to the molar bulk flow. Formation of more than one product species for the case without buffer gas would result in a reduction of the deposition rate.¹²

An analytical solution can be obtained for the limiting case of diffusive mass transport of A to a hemispherical surface of radius a followed by chemical reaction to form a gaseous species B.¹⁴ This same solution is valid for the case of diffusion of A through a buffer gas to a surface where chemical reaction takes place to form any number of reactants. From this solution, a radial growth rate for a hemispherical deposit can be derived, where v_1 is the volume of a deposited atom and k_1 is the first-order surface-reaction rate constant:

$$\frac{da}{dt} = \frac{k_1 p_1 v_1}{kT} \left(\frac{1}{1 + (ak_1/D_{AB})} \right) \quad (3)$$

At steady state and for low surface-reaction rates (small k_1), the deposition rate is limited by the surface reaction and is given by $k_1 p_1 v_1 / kT$. For high reaction rates, the deposition rate is given by eq 4 in Table I for diffu-

sion-limited deposition.⁷ This equation describes the deposition rate under quasi-steady-state conditions when the effects of free convection and thermal diffusion are negligible. The effect of including thermal diffusion is difficult to quantify, but would probably result in a reduction of calculated deposition rates below those obtained by using eq 4 (Table I).

Transition Regime

Only in the limiting cases of $Kn \gg 1$ and $Kn \ll 1$ is the theoretical description of transport to a reaction zone simple and well understood. For $Kn \sim 1$, the transition regime, a rigorous description of the transport phenomena requires solving the Boltzmann equation.¹⁶⁻¹⁸ The diffusion equation (eq 1) in particular becomes invalid, especially in the region of the reaction zone, for in this region $r - a \leq \delta$, where δ is on the order of the gas mean free path. In this region, molecular collisions do not occur and continuum theory breaks down. However, for $r - a \gg \delta$, transport occurs by diffusion. Thus, both diffusion and molecular bombardment are important in the overall problem.

The simplest semiempirical expression for the flux in the transition regime approaching eqs 2 and 4 (Table I) in the limits of large and small Kn was presented by Fuchs.¹⁵ The flow of molecules toward the deposit surface is assumed diffusive (and can be described by a diffusion equation similar to eq 1) up to an arbitrary distance δ from the surface. Inside this surrounding shell, transport is assumed to occur by free molecular flow. By matching the fluxes (diffusive and molecular) at the surface of this shell, Fuchs obtained the following expression for the flux to the surface:

$$J = J_K / \left(1 + \frac{a^2 \bar{v}}{4D_{AB}(a + \delta)} \right) \quad (5)$$

In this expression, J_K is the molecular flux due to transport by molecular bombardment while J is the diffusive flux, and \bar{v} is the average molecular velocity, $(8kT/\pi m)^{1/2}$. The main problem lies in the determination of a value for δ , a distance that cannot be determined theoretically. For $\delta = 0$, the simplest but most physically unrealistic choice, this result reduces to the interpolation eq 6 in Table I for the deposit growth rate. If the Knudsen number is defined by $Kn = 3D_{AB}/(a(8kT/\pi m)^{1/2})$, the interpolation formula reduces to eq 4 for $Kn/\alpha \ll 1$ and to eq 2 for $Kn/\alpha \gg 1$. Fuchs and Sutugin¹⁶ and Loyalka¹⁸ have developed alternate interpolation formulas. The Fuchs and Sutugin equation exhibits the proper limits in the continuum and free-molecule regimes and provides a method for calculating mass-transport rates for any values of the gas mean free path. The accuracy of their expression has been verified by studying mass-transport rates to aerosol particles for various values of the Knudsen number.^{13,19} It is important to note that these various interpolation formulas predict a similar dependence on the mean free path and deposit size.

(11) Herman, I. P.; Hyde, R. A.; McWilliams, B. M.; Weisberg, A. H.; Wood, L. L. *Mater. Res. Soc. Symp. Proc.* **1983**, *17*, 9.

(12) Skouby, D. C.; Jensen, J. F. *J. Appl. Phys.* **1988**, *63*, 198.

(13) Richardson, C. B.; Lin, H. B.; McGraw, R.; Tang, I. N. *Aerosol Sci. Technol.* **1986**, *5*, 103.

(14) Crank, J. *The Mathematics of Diffusion*; Clarendon Press: Oxford, 1975.

(15) Fuchs, N. A. *Evaporation and Droplet Growth in Gaseous Media*; Pergamon Press: New York, 1959.

(16) Fuchs, N. A.; Sutugin, A. G. *Highly Dispersed Aerosols*; Ann Arbor Science Publishers: Ann Arbor, MI, 1970.

(17) Sahn, D. C. *J. Nucl. Energy* **1966**, *20*, 915.

(18) Loyalka, S. K. *J. Chem. Phys.* **1973**, *58*, 354.

(19) Davis, E. J.; Ravindran, P.; Ray, A. K. *Adv. Colloid Interface Sci.* **1981**, *15*, 1.

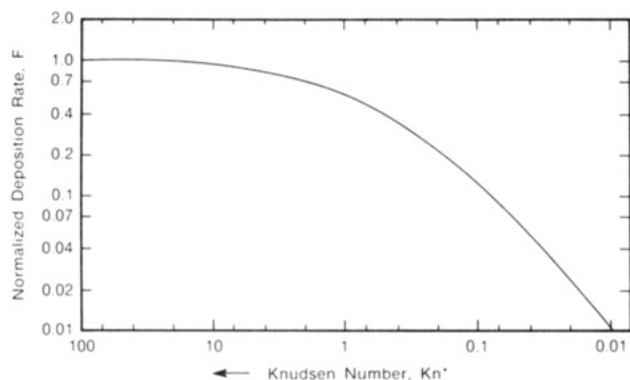


Figure 2. Vertical growth rate normalized with respect to maximum vertical growth rate as a function of Knudsen number and reaction probability α . Knudsen number and reaction probability determine the importance of diffusional resistance to mass transport.

In order to understand the influence of diffusion on the growth rate, the rate can be formulated in terms of the maximum vertical growth rate, by eq 2 (Table I). The ratio of the rate to the maximum deposition rate at $\text{Kn}/\alpha \gg 1$ is given by F :⁷

$$F = \frac{da/dt}{\alpha v_1 p_1 / (2\pi m k T)^{1/2}} = \frac{4(\text{Kn}^*)/3}{1 + 4(\text{Kn}^*)/3} \quad (7)$$

where $\text{Kn}^* = \text{Kn}/\alpha$. Figure 2 shows how the normalized deposition rate, F , depends on Kn^* . The normalized deposition rate depends on $D_{AB}/a\alpha$ or on $(p_{\text{tot}}\alpha)^{-1}$ since the diffusion coefficient D_{AB} depends inversely on the total pressure. Thus, the total pressure at which diffusional effects begin to decrease the deposition rate depends on α and the size of the deposit.

The deposit growth equations for mass-transport-controlled thermal LCVD (summarized in Table I) are applicable to a steady-state process. The validity of these equations has been experimentally demonstrated for the deposition of Au from $\text{Me}_2\text{Au}(\text{hfac})$ in the absence and presence of buffer gas.⁷ The behavior of the rate with respect to the total pressure, p_{tot} , and the partial pressure of the precursor, p_1 , can be ascertained: in the diffusion regime ($\text{Kn} \ll 1$), the rate is proportional to p_1 as in the $\text{Kn} \gg 1$ regime, but because of the dependence on D_{AB} , the rate is inversely proportional to p_{tot} . The relaxation time to steady state is negligible for $\text{Kn} \gg 1$, since in this limit the incoming gas molecules are not influenced by the presence of the deposition zone.²⁰

Diffusive transport can strongly influence the morphology and shape of deposits by controlling the rates of growth.^{12,21} Within the reaction zone, for example, there can be substantially different deposition or growth rates, resulting in nonhemispherical or irregularly shaped deposits. The effects of diffusion-limited deposition have been described for the growth of gold crystals during the thermal LCVD of gold.²¹ The addition of more than approximately 10 Torr of air or oxygen allowed the growth of gold deposits containing crystallites that grew out radially from the nucleated region and were much larger than those obtained in the

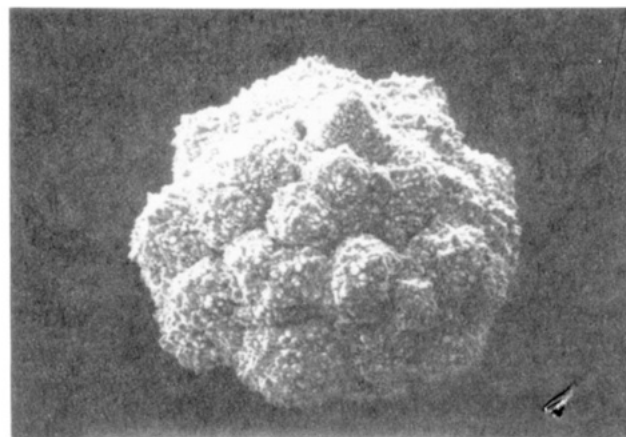


Figure 3. A hemispherical deposit structure of gold from LCVD with a stationary beam, obtained with 100-mW laser power on alumina with a beam diameter of approximately 10 μm .



Figure 4. A deposit of gold obtained under conditions of diffusional transport. The deposit was grown in the presence of 250 Torr of air and the vapor pressure of dimethyl gold hexafluoroacetylacetonate.

absence of buffer gas (see Figures 3 and 4).

Photochemical Deposition and Cluster Formation

Lasers can be used to drive photochemical reactions in the gas phase which result in the formation of reactive species or metal atoms that are then transported to the substrate or form clusters in the gas phase (see Figure 1). The rate of transport of the reactive species and metal atoms to the substrate can determine the shape of the deposit and the deposition rate. Similarly, the rates of transport to and from the irradiated zone can determine whether or not cluster formation occurs in the gas phase.

As for thermally induced deposition, the two limiting cases of $\text{Kn} \gg 1$ and $\text{Kn} \ll 1$ are considered here. $\text{Kn} \gg 1$ provides deposition by a ballistic process. No concentration profile exists in the gas phase, and the deposition rate does not depend on the diffusion coefficient. Thus, addition of buffer has no effect on the deposition rate as long as the gas mean free path

(20) Comita, P. B.; Kodas, T. T. *Appl. Phys. Lett.* **1987**, *51*, 2059.
Kodas, T. T.; Comita, P. B. *J. Appl. Phys.* **1988**, *65*, 2513.

(21) Kodas, T. T.; Baum, T. H.; Comita, P. B. *J. Cryst. Growth* **1988**, *87*, 378.

is long compared to the deposit size. This case has been analyzed by Wood et al.²² and Chen.²³ Their result (eq 8, Table I) can be compared to the corresponding result for thermally driven surface reactions (eq 2). For both cases, the deposition rate is proportional to the reactant concentration and α and does not depend on the diffusion coefficient. For the thermally driven case, however, the deposition rate does not depend on the radius of the laser beam, r , or the size of the reaction zone, a .

For $Kn \ll 1$, transport of species to the surface occurs by diffusion and a concentration gradient may exist in the gas phase. This situation has been analyzed by Krchnavek et al.²⁴ and Chen,²³ who solved eq 1 without convection at steady state. The deposition rate for this case is given by eq 9 (see Table I), which is just eq 8 modified by a factor of 2.²³ The rate for both cases depends on $1/a$, so that decreasing the size of the reaction zone increases the rate. In contrast to the result for thermally driven LCVD, the result for the photochemical process does not depend on the diffusion coefficient. The key difference is that thermally induced deposition is driven by a surface reaction which provides a sink for the reactant molecules. Changing the buffer-gas pressure does not change the concentration gradient in the gas phase, but decreases the diffusion coefficient. In the photochemical process, deposition is driven by a gas-phase reaction whose rate does not depend on the buffer-gas pressure. Adding buffer gas increases the concentration gradient and decreases the diffusion coefficient, resulting in only a small change in the transport rate. While few advantages exist for adding buffer gas during thermally driven processes, adding buffer gas for the case of photochemically driven processes can have the advantage of producing better resolution for the deposit. Adding Ar buffer gas during Al deposition, for example, can result in diffusion suppression resulting in narrower features.²⁵

Gas-Phase Particle Formation

The addition of buffer gas to a photochemical deposition system can also result in cluster formation in the gas phase. This particle-formation process can place an upper limit on the deposition rate since particle formation in the gas phase can have deleterious effects if the goal is deposition of a uniform adherent film. Powder formation occurs at high pressures and high gas-phase reaction rates, and this can be exploited in systems designed for powder generation.²⁶⁻⁴² Qualita-

tively, this behavior occurs because, as the pressure is increased, the concentration of the diffusing species in the gas phase increases. Similarly, increasing gas-phase reaction rates also results in an increase in the gas-phase concentration of the diffusing species. Above a critical concentration, collisions between atoms or molecules become frequent enough to result in particle formation.

The particle-formation process can be understood by examining eq 1. Consider the case of a cylindrical laser beam passing through a larger cylindrical chamber containing a reactive gas. The laser drives reactions that produce, in the simplest case, metal atoms, which can then diffuse to the walls of the vessel and deposit. Alternatively, the metal atoms can collide in the gas phase and nucleate to form particles. A variety of nucleation theories exist which have the common feature that they predict that the cluster-formation rate should be extremely sensitive to the gas-phase concentration of the metal atoms. Thus, for practical purposes, a critical value of the gas-phase metal atom concentration exists above which cluster formation occurs. Equation 1 can be solved to obtain an expression for the concentration in the gas phase, which can then be compared with this critical value.

Raes et al.²⁶ have examined this situation in detail by solving the full diffusive transport equation numerically and by solving a simplified version analytically. Their results were used to describe excimer laser and mercury arc lamp induced deposition with gas-phase photochemical reactions and cluster formation. The analytical results in these studies can be used to gain insight into the parameters that control particle formation in systems with laser-driven reactions. The solution for the product concentration along the axis of the laser beam (the region where the product concentration is at a maximum) can be obtained by solving eq 1 under the assumptions stated above and is given by⁴² $C = R\omega^2G/4D_{AB}$. In this equation, C is the concentration of the diffusing species, R is the rate of formation of the diffusing species, ω is the diameter of the laser beam, D_{AB} is the diffusion coefficient of the diffusing species in the buffer gas, and G is a geometrical factor. Adding buffer gas to the system reduces the diffusion coefficient and results in a higher concentration of the reactive species in the gas phase within the beam. This in turn results in particle formation along the axis of the laser beam. Similarly, increasing either the radius of the laser beam or the reaction rate increases the concentration and can result in particle formation. The critical value of the concentration required for particle formation depends on the nature of the particle-formation process and depends on the particular species involved.

(22) Wood, T. H.; White, J. C.; Thacker, B. A. *Appl. Phys. Lett.* **1983**, *42*, 408.

(23) Chen, J. C. *J. Vac. Sci. Technol.*, **A** **1988**, *5*, 3386.

(24) Krchnavek, R. R.; Gilgen, H. H.; Chen, J. C.; Shaw, P. S.; Licata, T. J.; Osgood, R. M. *J. Vac. Sci. Technol. B* **1987**, *5*, 20.

(25) Arai, Y.; Yamaguchi, S.; Ohsaki, T. *Appl. Phys. Lett.* **1988**, *52*, 2083.

(26) Raes, F.; Kudas, T. T.; Friedlander, S. K. *Aerosol Sci. Technol.*, in press.

(27) Love, P. J.; Loda, R. T.; La Roe, P. R.; Green, A. K.; Rehn, V. *Mater. Res. Soc. Symp. Proc.* **1984**, *29*, 101.

(28) Meunier, M.; Gattuso, T. R.; Adler, D.; Haggerty, J. S. *Appl. Phys. Lett.* **1983**, *43*, 273.

(29) Meunier, M.; Flint, J. H.; Adler, D.; Haggerty, J. S. *J. Non-Cryst. Solids* **1983**, *59/60*, 699.

(30) Bilenchi, R.; Gianinoni, I.; Musci, M. *J. Appl. Phys.* **1982**, *53*, 6479.

(31) Bilenchi, R.; Gianinoni, I.; Musci, M.; Murri, R.; Tacchetti, S. *Appl. Phys. Lett.* **1985**, *47*, 279.

(32) Scott, B. A.; Plecenik, R. M.; Simonyi, E. E. *Appl. Phys. Lett.* **1981**, *39*, 73.

(33) Pauleau, Y.; Tonneau, D.; Auvert, G. *Laser Processing and Diagnostic*. Bauerle, D., Ed. *Springer Ser. Chem. Phys.* **1984**, *39*, 215.

(34) Pauleau, Y.; Stawski, R.; Lami, P.; Auvert, G. *Mater. Res. Soc. Symp. Proc.* **1984**, *29*, 41.

(35) Jasinski, J. M.; Estes, R. D. *Chem. Phys. Lett.* **1985**, *117*, 495.

(36) Jasinski, J. M.; Meyerson, B. S.; Ngyuen, T. N. *J. Appl. Phys.* **1987**, *61*, 431.

(37) Tonneau, D.; Auvert, G.; Pauleau, Y. *J. Vac. Sci. Technol.*, **A** **1986**, *4*, 670.

(38) Gattuso, T. R.; Meunier, M.; Addler, D.; Haggerty, J. S. *Mater. Res. Soc. Symp. Proc.* **1983**, *17*, 215.

(39) Hanabusa, M.; Moriyama, S.; Kikuchi, H. *Thin Solid Films* **1983**, *107*, 227.

(40) Hanabusa, M.; Kikuchi, H. *Jpn. J. Appl. Phys.* **1983**, *22*, L712.

(41) Flynn, D. K.; Steinfeld, J. I.; Sethi, D. S. *J. Appl. Phys.* **1986**, *59*, 3914.

(42) Kudas, T. T.; Pratsinis, S. E.; Friedlander, S. K. *J. Colloid Interface Sci.* **1986**, *111*, 102.

The particle-formation process has been examined by a number of investigators in detail. Particle formation at high pressures has been observed in the photochemical deposition of metal atoms such as Fe, Cr, Mo, and W^{27,42,43} and can result in poor adhesion of films to the substrate.⁴² Particle formation has also been observed during deposition of hydrogenated amorphous silicon from SiH₄ under a wide variety of conditions.²⁸⁻⁴⁰ A study of the formation of UF₆ particles using a dye laser showed that a critical minimum pressure of the reactant was required to obtain particle formation,⁴⁴ a process that can be used as the basis for isotope separation.⁴⁵ Particle formation,⁴⁶ nucleation kinetics,⁴⁷ aerosol dynamics,⁴⁸ and film generation⁴⁹ have been examined for a variety of processes, and the studies generally show

(43) Draper, C. *Metall. Trans.* 1980, 11A, 349.

(44) Borsella, E.; Catoni, F.; Freddi, G. *J. Chem. Phys.* 1980, 73, 316.

(45) Ronn, A.; Earl, B. *Chem. Phys. Lett.* 1977, 45, 556.

(46) Yabuzaki, T.; Sato, T.; Ogawa, T. *J. Chem. Phys.* 1980, 73, 2780.

(47) Lin, S.; Ronn, A. *Chem. Phys. Lett.* 1978, 56, 414.

(48) Sato, T.; Yabuzaki, T.; Ogawa, T. *Jpn. J. Appl. Phys.* 1982, 21, 1599.

(49) Jervis, T.; Menon, S.; Joyce, E.; Carrol, D. *Mater. Res. Soc. Symp. Proc.* 1987, 75, 159.

that the conditions required for generation of adherent films, without cluster formation, are low pressures, low reaction rates, and a small laser-beam diameter.

Concluding Remarks

We have attempted to provide a framework for understanding the effects of mass transport on the rates of physical and chemical processes occurring in laser-induced surface and gas-phase reactions. The fundamental interest in this area is related to the rate at which a focused laser can drive a localized chemical reaction, either in the gas phase or on a surface, and the physical limitations to this rate. The relationship between the size of the reaction zone, the mean free path in the gas phase, and the rate of gas-phase and surface reactions provides the key to the understanding of the rate phenomena. Both thermally driven reactions and photochemical reactions are influenced by these size effects. Many of the consequences of mass transport in laser-induced reactions, such as control of deposit growth rate, deposit shape, crystal morphology, and other material properties, are just now beginning to be understood.

Environmental Behavior of Chlorinated Dioxins and Furans

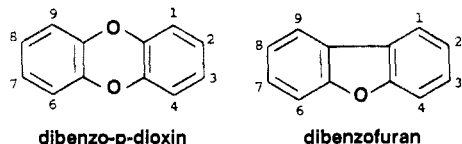
RONALD A. HITES

School of Public and Environmental Affairs and Department of Chemistry, Indiana University, Bloomington, Indiana 47405

Received January 18, 1990 (Revised Manuscript Received March 26, 1990)

Introduction

Chlorinated dibenzo-*p*-dioxins (called dioxins in this Account) and dibenzofurans (furans) are well-known environmental contaminants. The United States has spent billions of dollars studying these compounds. They have received public attention at the highest levels from several governments. It would be hard to name another class of compounds with a similar reputation.



Most of this public scrutiny has been caused by one member of this class: 2,3,7,8-tetrachlorodibenzo-*p*-dioxin (2378-D). This compound is known as "the most toxic man-made chemical". It takes only 0.6 μg of 2378-D/kg of body mass to kill 50% of a population of guinea pigs.¹ 2,3,7,8-Tetrachlorodibenzofuran (2378-F) is almost as toxic.² Clearly, the dioxins and furans are

hazardous compounds that warrant concern. Luckily, things are not as bad as they might seem. The toxicity of 2378-D to guinea pigs is not typical. There is a wide range of sensitivities among various animal species; for example, most hamsters will not die until the dose of 2378-D reaches 5000 μg kg⁻¹, a dose 10⁴ times higher than for guinea pigs.³ Furthermore, dioxins and furans in which the chlorine atoms are at different positions on the rings are not nearly as toxic; for example, 1368-D is >10⁶ times less toxic than 2378-D.⁴

These compounds came to the widespread attention of chemists (and to some extent the public) in 1973 when Baughman and Meselson pointed out that 2378-D was a contaminant in Agent Orange, a material used to kill vegetation in South Vietnam as part of a strategy by the U.S. Army to deny the Vietcong hiding places in the jungle.⁵ Agent Orange consisted of a mixture of (2,4-dichlorophenoxy)- and (2,4,5-trichlorophenoxy)acetates; the latter was made from 2,4,5-trichlorophenol that contained low concentrations of 2378-D. This impurity was carried over into the Agent Orange, and as a result, 2378-D was delivered into the ecosystem of Vietnam. Baughman and Meselson raised questions,

(1) Sparschu, G. L.; Dunn, F. L.; Rowe, V. K. *Food Cosmet. Toxicol.* 1971, 9, 405.

(2) Moore, J. A.; McConnell, E. E.; Dalgard, D. W.; Harris, M. W. *Ann. N.Y. Acad. Sci.* 1979, 320, 151-163.

(3) Kociba, R. J.; Schwertz, B. A. *Drug Metab. Rev.* 1982, 13, 387-406.

(4) Kociba, R. J.; Cabey, O. *Chemosphere* 1985, 14, 649-660.

(5) Baughman, R.; Meselson, M. *Environ. Health Perspect.* 1973, *Experimental Issue No. 5*, 27-35.

Ron Hites was born in Michigan in 1942. He received a B.A. in Chemistry from Oakland University (near Detroit) in 1964 and a Ph.D. in Analytical Chemistry with Klaus Blemann from the Massachusetts Institute of Technology (MIT) in 1968. He remained on the staff and faculty of MIT until 1979, when he became a Professor of Public and Environmental Affairs at Indiana University; he is also a Professor of Chemistry. Last year he was elevated to the rank of Distinguished Professor. His research focuses on the behavior of potentially toxic organic compounds in the environment. He is currently President of the American Society for Mass Spectrometry.